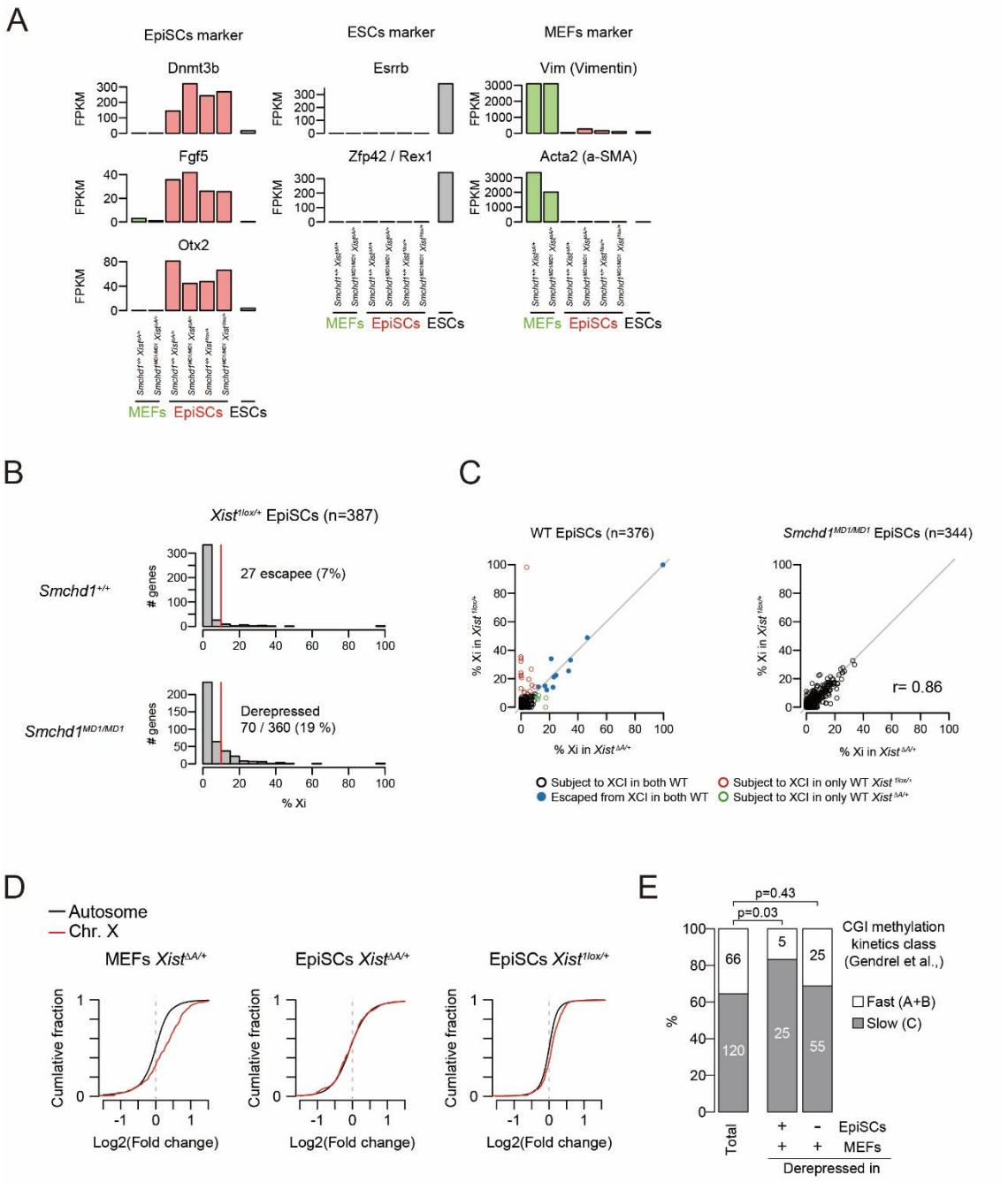

Fig. S1. Effect of SmcHD1-deficiency on X-inactivated genes was essentially the same between *Xist*$^{\Delta A}$/+ and *Xist*^{1lox}/+ background in EpiSCs.

(A) Expression levels of marker genes for EpiSCs, ESCs, and MEFs were compared in EpiSCs and MEFs with respective genotypes.

(B) Histograms showing the numbers of genes with the respective scores of Xi-probability in wild-type (top) and *Smchd1*$^{MD1/MD1}$ (bottom) EpiSCs on *Xist*^{1lox}/+ background.

(C) Comparison of the degree of derepression for X-linked genes on the Xi between *Xist*$^{\Delta A}$/+ and *Xist*^{1lox}/+ background. (left) Of 376 informative genes in all 4 relevant EpiSC lines, 344 genes (black open circles) were silenced on the Xi and 11 genes (blue filled circles) were escaped from XCI in both wild-type EpiSC lines. Sixteen (red open circles) and 5 (green open circles) genes were classified as escapees in wild type on *Xist*^{1lox}/+ and *Xist*$^{\Delta A}$/+ background, respectively. (right) Although the number of escaped genes in wild type was larger on *Xist*^{1lox}/+ background than on *Xist*$^{\Delta A}$/+, 344 commonly silenced genes were similarly derepressed in *Smchd1*$^{MD1/MD1}$ on both *Xist* background (Pearson correlation coefficient, r = 0.86).

(D) Cumulative distribution plot of fold-changes of expressed X-linked genes (red) versus autosomal genes (black) between wild-type and *Smchd1*$^{MD1/MD1}$ in MEFs and respective EpiSCs lines as indicated.

(E) Comparison between CGI methylation kinetics in differentiating XX embryonic stem cells (Gendrel et al., 2012) and derepression statuses in EpiSCs and MEFs. Percentage of genes associated with slow-methylating CGIs are shown with the number of genes in the boxes. Among 186 genes with the CGI methylation kinetics, class A+B (n=120) and C (n=66) genes are associated with fast- and slow-methylating CGIs, respectively, according to the definition by Gendrel et al. (2012). p-value, chi-squared test.

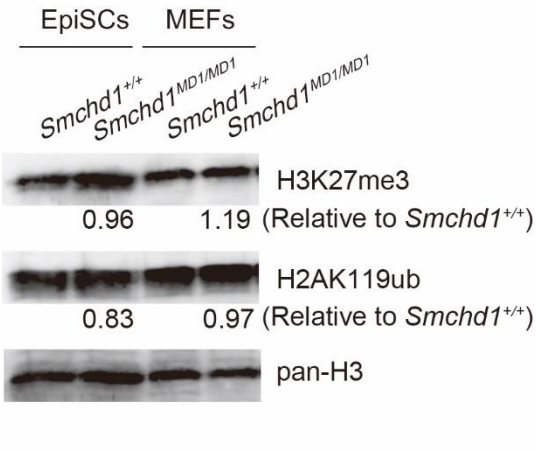

Fig. S2. Global levels of histone modifications in EpiSCs and MEFs.

Western blot analysis showing global levels of H3K27me3 and H2AK119ub in wild-type and *Smchd1*$^{MD1/MD1}$ EpiSCs and their respective counterparts in MEFs. Relative abundance of respective histone modifications in *Smchd1*$^{MD1/MD1}$ to wild type cells is shown below the band. Twenty micrograms of whole cell lysate was loaded.

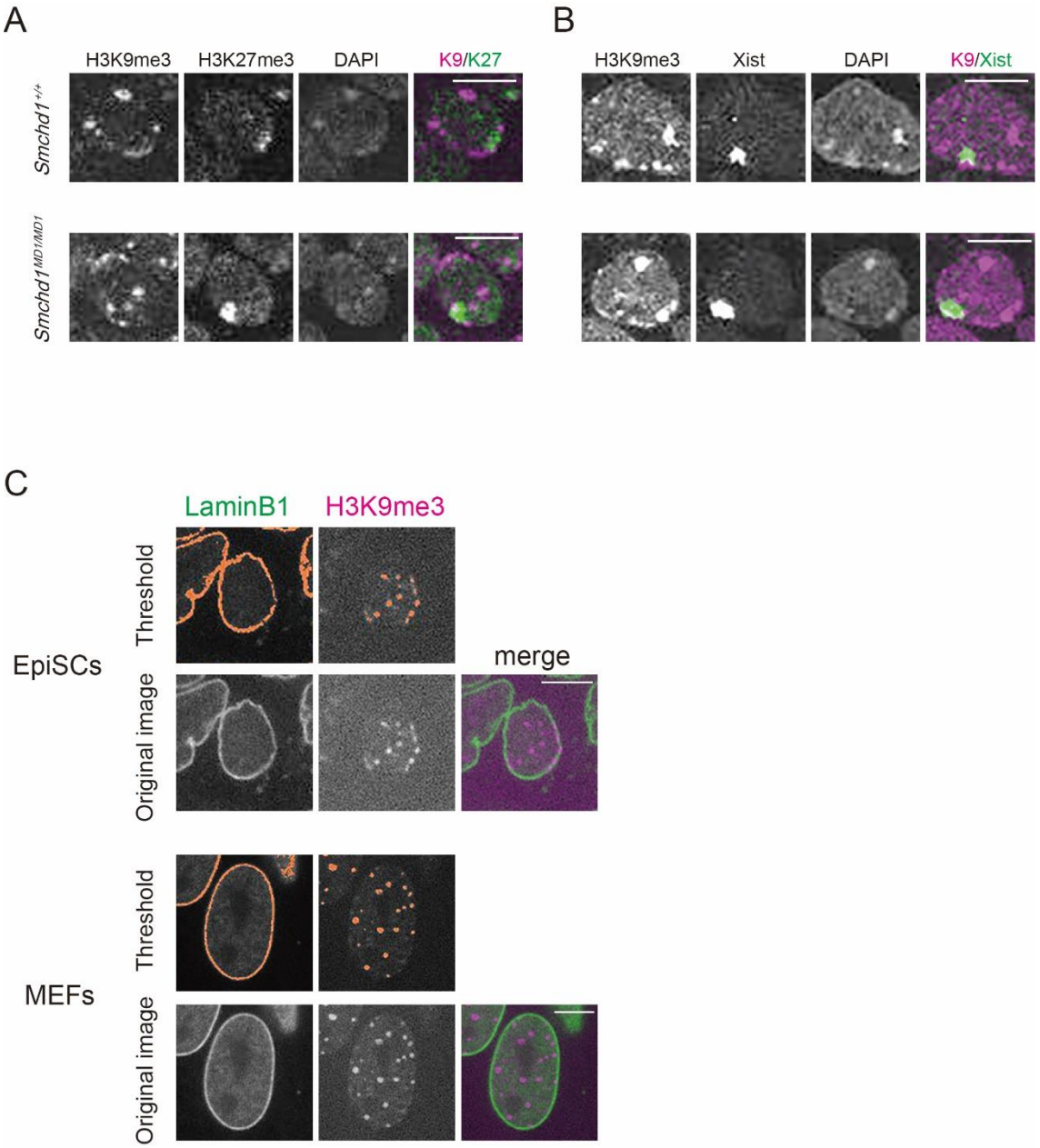

Fig. S3. Immunofluorescence of H3K9me3 and H3K27me3 in wild-type and *Smchd1*$^{MD1/MD1}$ EpiSCs.

(A) Immunofluorescence of wild-type and *Smchd1*$^{MD1/MD1}$ EpiSCs and MEFs for H3K9me3 (magenta) in combination with H3K27me3 (green). Images are one of nuclei in respective cells as indicated on a single plane. Scale bar, 10 μm.

(B) Immuno-RNA-FISH of wild-type and *Smchd1*$^{MD1/MD1}$ EpiSCs for H3K9me3 (magenta) and *Xist* RNA (green). Images are one of nuclei in respective cells as indicated on a single plane. Scale bar, 10 μm.

(C) How the extent of colocalization of fluorescence for H3K9me3 and Lamin B1 was quantified is shown. Threshold manually set for LaminB1 and H3K9me3 in each nucleus is shown in orange. Scale bar, 10 μm.

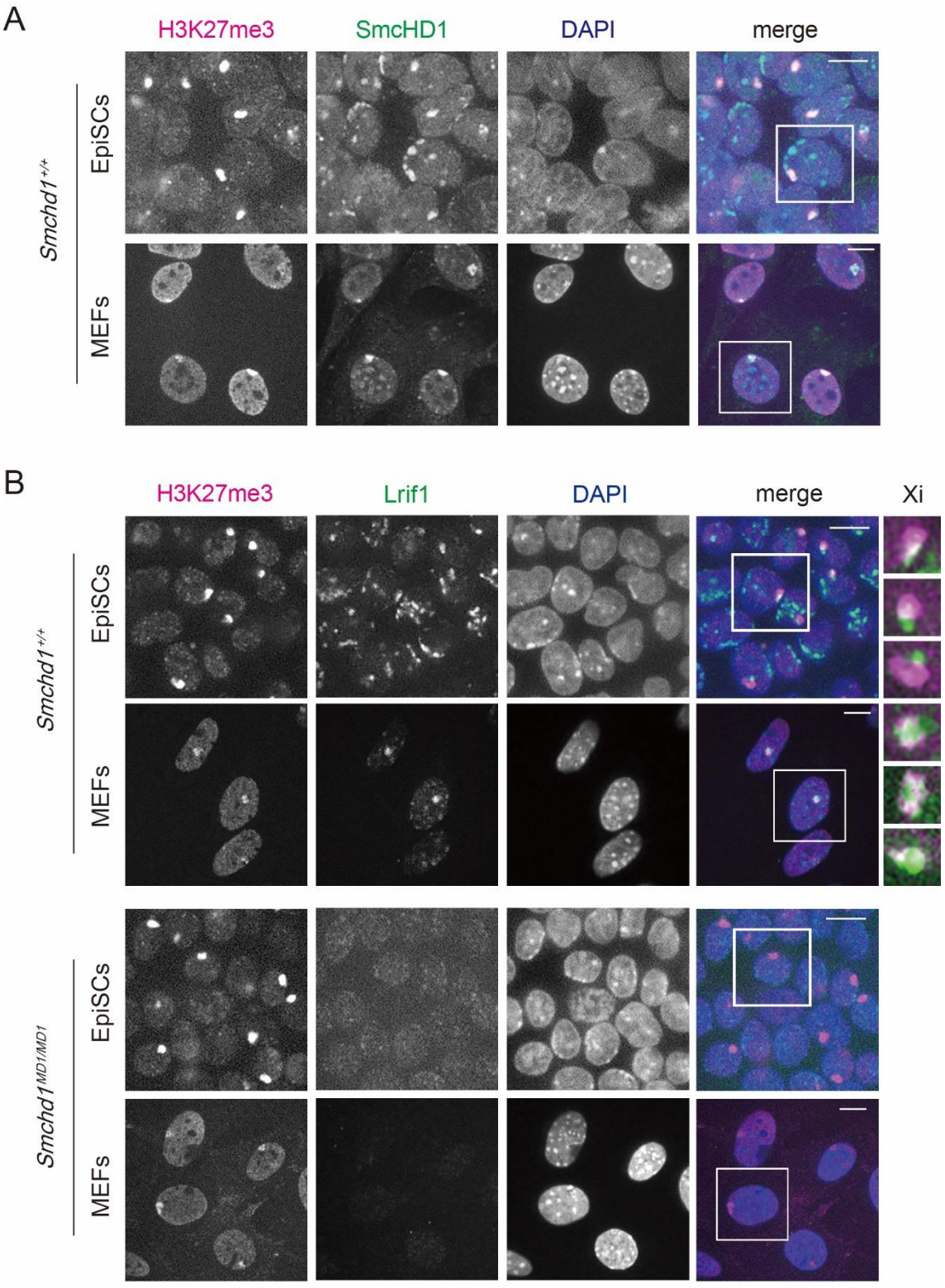

Fig. S4. Immunofluorescence of SmcHD1 and Lrif1 in EpiSCs and MEFs.

(A) A wider view of the field surrounding the nucleus shown in Figure 4A. The nucleus shown in Figure 4A is indicated by a rectangle in the merged image. Scale bar, 10 μm.

(B) A wider view of the field surrounding the nucleus shown in Figure 4B. The nucleus shown in Figure 4C is indicated by a rectangle in the merged image. Scale bar, 10 μm. Rightmost three panels are blowups showing the localization of H3K27me3 (magenta) and Lrif1 (green) at the Xi domain. Their overlap appears in white.

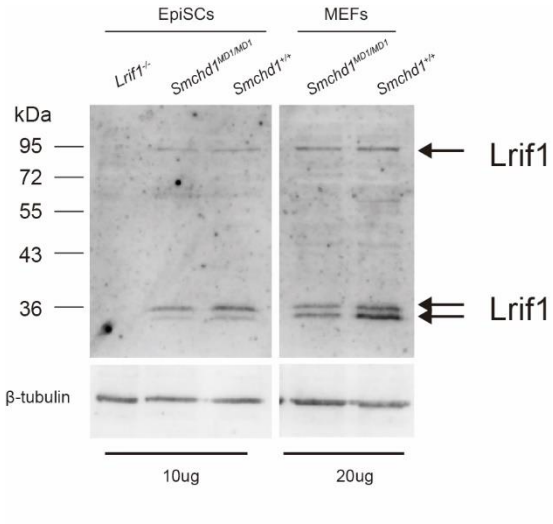

Fig. S5. Western blotting of Lrif1.

Western blot showing Lrif1 expression in wild-type and *Smchd1*$^{MD1/MD1}$ EpiSCs (left) and those in wild-type and *Smchd1*$^{MD1/MD1}$ MEFs (right). Long and short isoforms were detected.

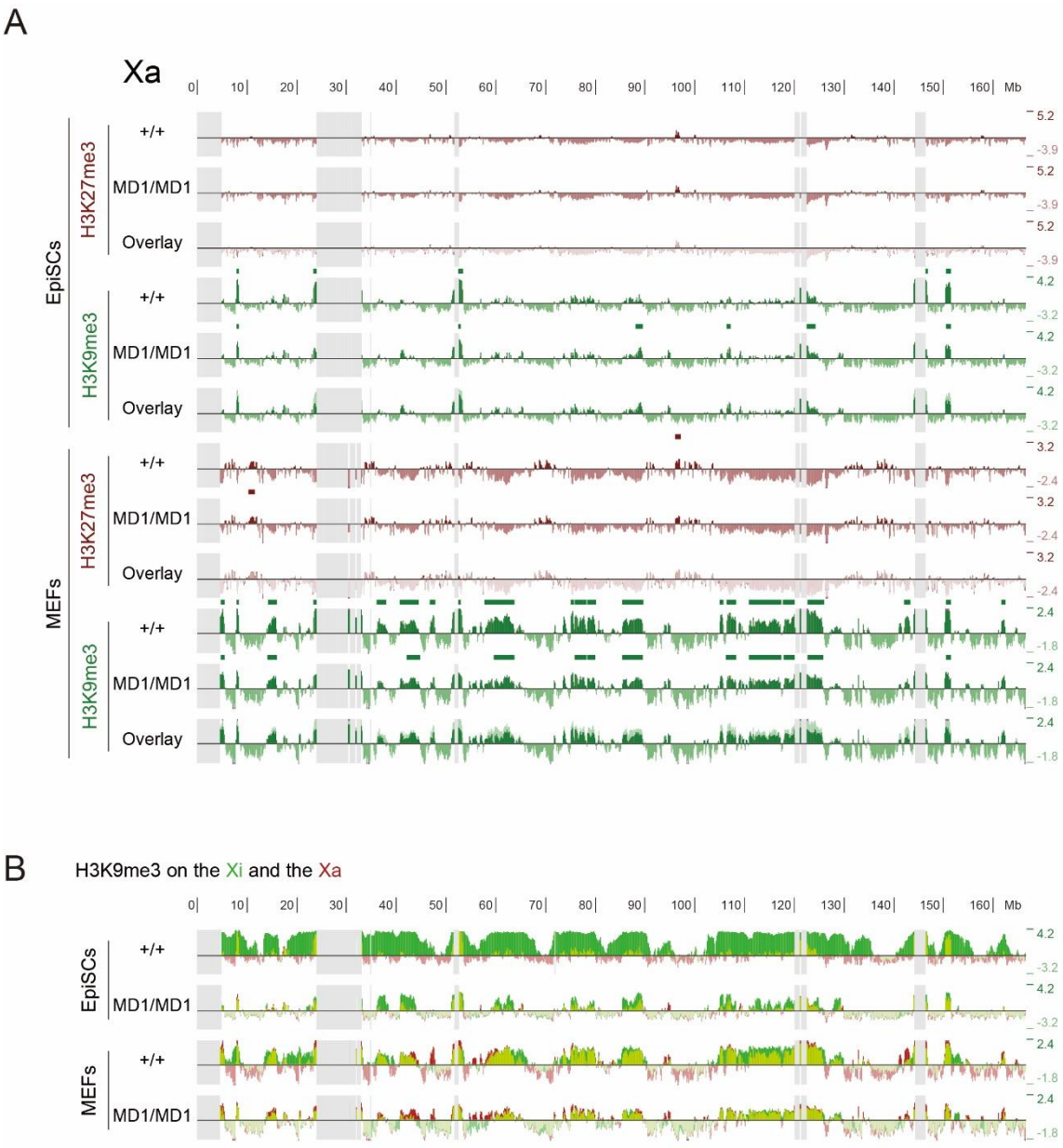

Fig S6. Histone modification states of the Xa in wild-type and *Smchd1*$^{MD1/MD1}$ EpiSCs and MEFs.

(A) Distribution of H3K9me3 and H3K27me3 on the Xa in wild-type and *Smchd1*$^{MD1/MD1}$ EpiSCs in comparison with that in the respective MEFs revealed by ChIP-seq. Each track and EDD domains are shown as Figure 6A.

(B) Overlay of H3K9me3 tracks of the Xa (red) and Xi (green) in the mutant EpiSCs and MEFs in comparison with that in the respective wild type.

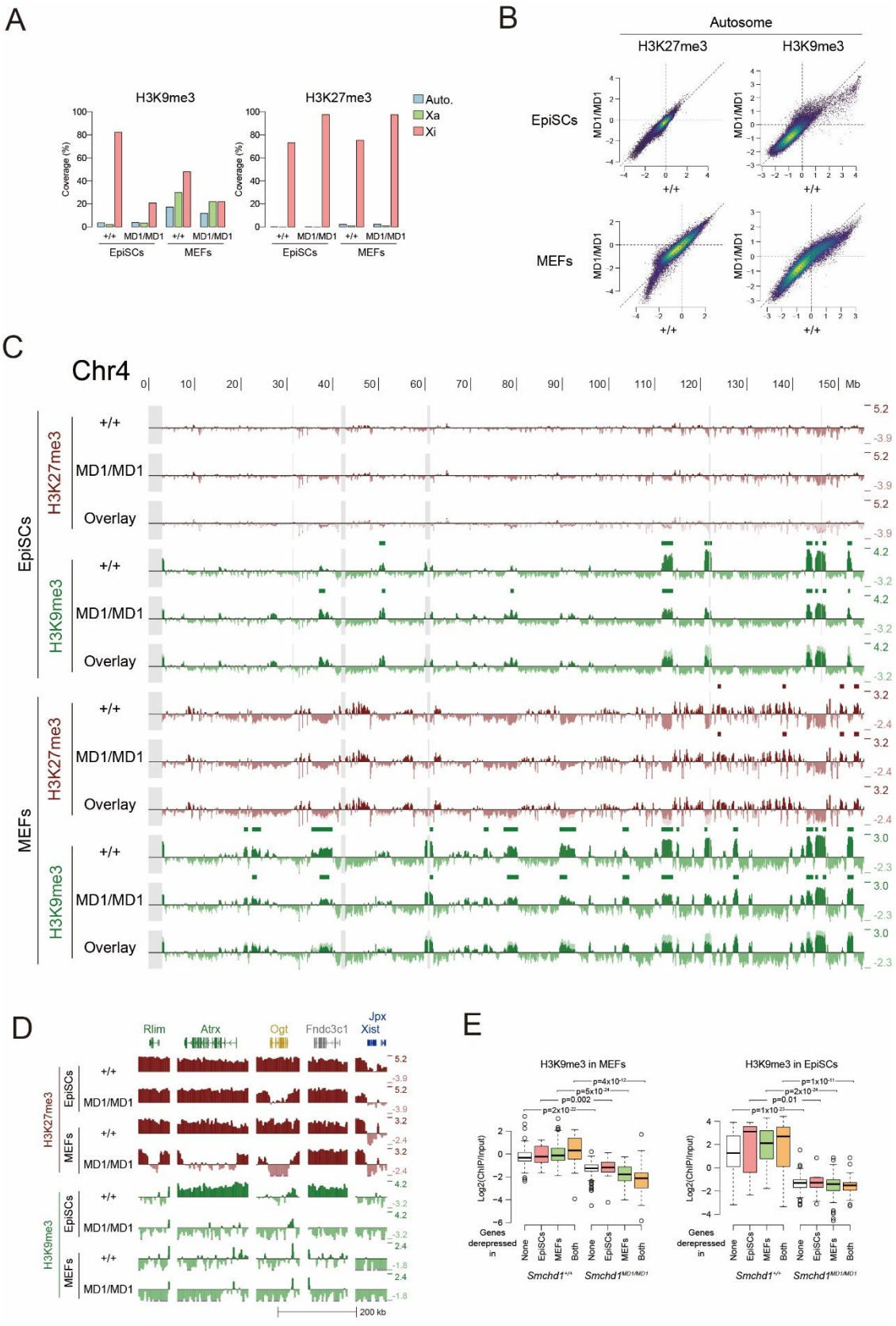

Fig. S7. Effect of SmcHD1-deficiency on H3K9me3.

(A)The EDD-domain coverages of H3K9me3 and H3K27me3 on the Xi in comparison with those on the Xa and autosomes in EpiSCs and MEFs. Note that only mappable genomic regions were considered.

(B)Scatter plot showing pairwise comparison of H3K27me3 (left) and H3K9me3 (right) enrichment within 50-kb windows across autosomes between wild-type and *Smchd1*$^{MD1/MD1}$ cells of EpiSCs (top) and MEFs (bottom).

(C)Histone modification states of chromosome 4 revealed by ChIP-seq in wild-type and *Smchd1*$^{MD1/MD1}$ EpiSCs and MEFs. Each track and EDD domains are shown as Figure 6A.

(D)Distribution of H3K27me3 and H3K9me3 per 5 kb bin at representative loci among different categories of genes on the Xi in EpiSCs and MEFs. *Rlim* and *Atrx* belong to those repressed in EpiSCs but derepressed in MEFs in the absence of SmcHD1. *Ogt* belongs to those commonly derepressed, *Fndc3c1* to those stably repressed, and *Xist* and *Jpx* to those that escape XCI in both mutant EpiSCs and MEFs.

(E)Box plot showing H3K9me3 enrichment within gene bodies for each group of genes classified in Figure 2B according to the state of derepression (MEF-specific, EpiSC-specific, both, and not derepressed) in MEFs and EpiSCs. The color of each box matches the color of each group in the Venn diagram shown in Figure 2B and D. p-value, Wilcoxon test (paired, one-sided).

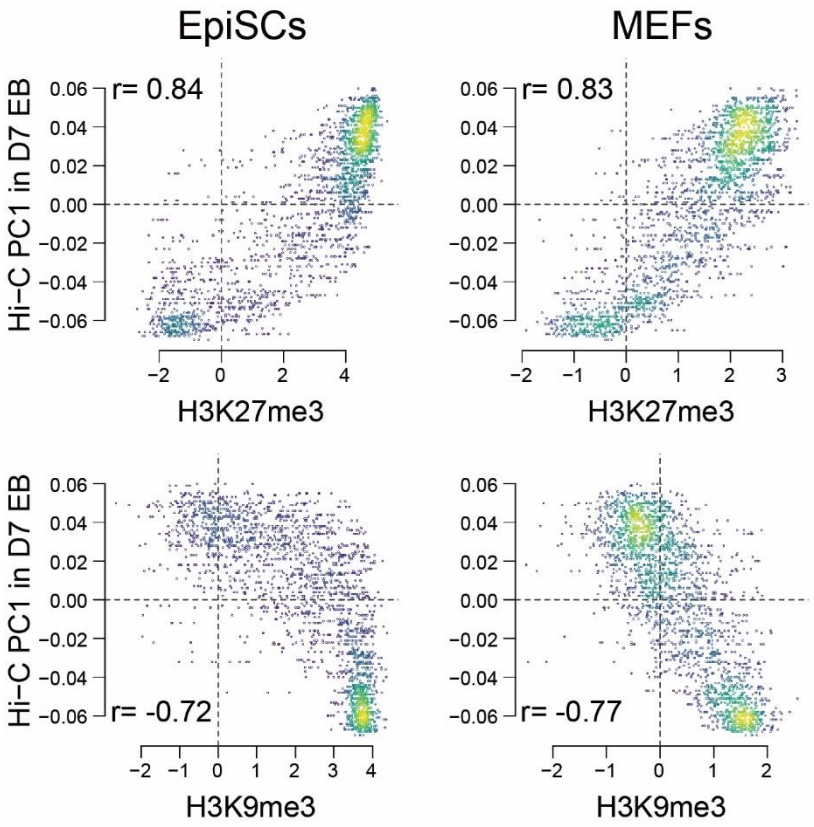

Fig. S8. A correlation between enrichment of histone modifications and PC1 of Hi-C data reported by Wang et al. (2018).

Scatter plot shows a pairwise comparison between enrichment of H3K27me3 in either EpiSCs or MEFs and PC1 of Hi-C in day 7 of EBs (Wang et al., 2018) (top) and between enrichment of H3K9me3 in either EpiSCs and MEFs and PC1 of Hi-C in day 7 of EBs (bottom).

Table S1. Genes classified as escapees in any of the three Smchd1^+/+ lines. The %Xi value highlighted by blue indicates the gene escaping XCI in the corresponding cell line. The references used for the known escapees are:

[1] Peeters et al., Bioessay 2014: Review
[2] Berletch et al., PLoS Genet 2015: escapees are defined from three mouse somatic tissues: brain, spleen and ovary.
[3] Marks et al., Genome Biol 2015: escapees are defined from three mNPC lines.
[4] Andergassen et al., Elife 2017: escapees are defined from 19 female mouse tissues

name	chrom	start	end	strand	% Xi in MEF Xist^ΔA/+	% Xi in EpiSCs Xist^ΔA/+	% Xi in EpiSCs Xist^1lox/+	known escapee? (references)
Gpkow	chrX	7274259	7287385	+	0.7	7.8	15.4	Yes (3)
Tfe3	chrX	7339786	7352328	+	0.1	6.4	11.3	Yes (3)
Gm6787	chrX	7674212	7683827	+	14.3		0.0	
Ddx3x	chrX	12858147	12871109	+	24.7	34.8	33.1	Yes (1,2,3,4)
Fundc1	chrX	17133694	17149423	-	0.5	23.1	21.2	
Kdm6a	chrX	17739792	17856484	+	31.5	46.5	48.8	Yes (1,2,3,4)
Slc9a7	chrX	19682880	19868890	-	0.0	10.0	0.0	Yes (4)
Zcchc12	chrX	33735898	33739153	+	0.0	0.0	13.1	
Ccdc160	chrX	50144376	50152645	+	11.8	8.6	1.9	Yes (4)
Tmem47	chrX	78315982	78343214	+	0.2	5.6	19.6	Yes (2,4)
Arhgef9	chrX	92244273	92361878	-	1.3	7.3	26.7	
Zc4h2	chrX	92834532	92853848	-	0.4	2.3	10.8	
Stard8	chrX	96237919	96270067	+	1.2	0.0	35.3	Yes (4)
Efnb1	chrX	96331468	96344330	+	0.9	0.0	32.1	
Kif4	chrX	97821403	97922610	+	0.0	0.0	21.9	Yes (2)
Snx12	chrX	98293124	98417902	-	0.4	0.4	20.6	Yes (4)
Nhsl2	chrX	99044723	99287394	+	0.0	11.9	5.6	Yes (4)
Xist	chrX	100655711	100678572	-	99.8	99.5	99.9	Yes (2,3,4)
Jpx	chrX	100688914	100701764	+	4.8	18.2	12.1	Yes (1,2,3)
Ftx	chrX	100756248	100819093	-	20.0	16.9	14.9	Yes (2,3,4)
5530601H04Rik	chrX	102236192	102265463	-	37.7	22.5	14.0	Yes (1,2,3)
Pbdc1	chrX	102275094	102312429	+	12.6	24.6	22.4	Yes (1,2,3,4)
Hmgn5	chrX	106199875	106208719	-	0.0	0.0	34.1	
Rps6ka6	chrX	108501445	108651568	-	0.6	0.2	22.4	Yes (4)
Chm	chrX	110154200	110299124	-	0.6	4.0	98.1	Yes (3)
Klhl4	chrX	111587941	111674738	+		21.2	33.9	
C330013F16Rik	chrX	135774764	135892277	-		17.3	0.0	
Tbc1d8b	chrX	136219534	136288757	+	0.0	17.6	6.5	Yes (4)
Psmd10	chrX	137482963	137491250	-	0.0	2.5	10.1	
Atg4a	chrX	137491455	137598813	+	0.1	12.3	14.3	Yes (4)
Col4a6	chrX	137599945	137908619	-	0.0	0.0	24.1	
Tmem29	chrX	146832315	146893693	-	16.0	9.8	9.2	Yes (2,3)
Kdm5c	chrX	148667769	148713642	+	30.3	33.4	25.4	Yes (1,2,3,4)
Foxr2	chrX	149553330	149567404	+		11.2	6.7	
Klf8	chrX	149672587	149830677	+	0.0	12.5	8.1	
Mid1	chrX	166123130	166428729	+	3.1	9.9	14.3	Yes (1,2,3)

Supplementary References

Andergassen, D., Dotter, C. P., Wenzel, D., Sigl, V., Bammer, P. C., Muckenhuber, M., Mayer, D., Kulinski, T. M., Theussl, H.-C., Penninger, J. M., et al. (2017). Mapping the mouse Allelome reveals tissue-specific regulation of allelic expression. *Elife* **6**, e25125. doi:10.7554/eLife.25125

Berletch, J. B., Ma, W., Yang, F., Shendure, J., Noble, W. S., Disteche, C. M. and Deng, X. (2015). Escape from X inactivation varies in mouse tissues. *PLOS Genetics* **11**, e1005079. doi:10.1371/journal.pgen.1005079

Marks, H., Kerstens, H. H. D., Barakat, T. S., Splinter, E., Dirks, R. A. M., Mierlo, G. van, Joshi, O., Wang, S.-Y., Babak, T., Albers, C. A., et al. (2015). Dynamics of gene silencing during X inactivation using allele-specific RNA-seq. *Genome Biol.* **16**, 149. doi:10.1186/s13059-015-0698-x

Peeters, S. B., Cotton, A. M. and Brown, C. J. (2014). Variable escape from X chromosome inactivation: identifying factors that tip the scales towards expression. *BioEssays* **36**, 746-756. doi:10.1002/bies.201400032

Table S2. List of primers used for genotyping, RT-PCR and qPCR

Allele	Primer seqnence(5'-3')
genotyping	
Smchd1^{+}	Fwd: tcaataggtccccctcatca Rev: tggacgatcagctttgggtg
Smchd1^{MD1}	Fwd: tcaataggtccccctcatca Rev: tggacgatcagctttgggta
Xist^{+}	Fwd: cggggcgcttggtggatggaaat Rev: gcaggtcgagggacctaata
Xist$^{\Delta A}$	Fwd: cggggcgcttggtggatggaaat Rev: gcacaaccccgcaaatgcta
Xist^{+2}	Fwd: gatgccaacgacacgtctga Rev: aaggactccaaagtaacaattca
Xist^{1lox}	Fwd: gatgccaacgacacgtctga Rev: cttagcgcagaagtcatgcc
allelic expression	
Rbm3	Fwd: gccttggtgctaattattgcc Rev: caaggacatcgcaatccttta
Pdha1	Fwd: ttccagcgatatgctgacttt Rev: tggcaaggcatgaagtgata
G6pd	Fwd: ttctagttcctgggcttgga Rev: ttaatggcagggttgggata
Hprt	Fwd: tgtggccatctgcctagtaa Rev: cagccaacactgctgaaaca
Rex3	Fwd: tagatgggacctgatgcaga Rev: gaagctggtaacagggagaga
qPCR	
Rnf12	Fwd: tcggagaaccagagcaagag Rev: tcacatggtgccgggttcta
Hprt	Fwd: gcctaagatgagcgcaagttg Rev: tactaggcagatggccacagg

Table S3. List of antibodies used for ChIP, Immunofluorescence and western blotting

antibody	source	identifier
anti-H3K27me3	Wako	MABI0323
anti-H3K27me3	Cell Signaling	9733T
anti-H3K9me3	Wako	MABI0308
anti-H3	Wako	MABI0301
anti-H2AK119ub	Cell Signaling	8240S
anti-SmcHD1	Sado-lab	Sakakibara et al., 2018
anti-Lrif1	This study	N/A
anti-beta-tubulin	Merk	05-661
anti-LaminB1	MBL	PM064